PAPER • OPEN ACCESS

Non-uniform heating effects in thermally developing turbulent pipe flows

To cite this article: Jonathan Neuhauser *et al* 2026 *J. Phys.: Conf. Ser.* **3173** 012040

View the article online for updates and enhancements.

You may also like

- A study on the influence of triggering pipe flow regarding mean and higher order statistics
F Zimmer, E -S Zanoun and C Egbers

- The response of hot wires in high Reynolds-number turbulent pipe flow
J D Li, B J McKeon, W Jiang et al.

- Recent progress in understanding the transition to turbulence in a pipe
R R Kerswell

Non-uniform heating effects in thermally developing turbulent pipe flows

Jonathan Neuhauser[1], Leo Bürk, Davide Gatti[1] and Bettina Frohnapfel[1]

[1]Institute of Fluid Mechanics, Karlsruhe Institute of Technology, Karlsruhe, Germany

E-mail: jonathan.neuhauser@kit.edu

Abstract. An analytical and numerical investigation of turbulent pipe flows in the thermal development region subject to an inhomogeneous heat flux distribution around the circumference has been conducted. We show analytically that the mean heat transfer (global Nusselt number Nu) does not depend on how the heat flux is distributed around the circumference. Hence, existing correlations for Nu remain applicable for azimuthally inhomogeneous heating. We present well-resolved numerical data for the thermal entrance region of non-uniformly heated pipe flows at different Prandtl (0.025, 0.71) and bulk Reynolds (5300, 19000) numbers. We show that, while the global Nu is unaffected by azimuthally inhomogeneous heating, the pointwise temperature has a much longer development length compared to a case with homogeneous heat flux. The development length is governed primarily by the azimuthal wavenumber $k = 1$ in the boundary condition.

1 Introduction

The global heat transfer properties of turbulent pipe flows are generally well understood; standard engineering correlations for the heat transfer properties exist for a wide range of Prandtl (Pr) and Reynolds (Re) numbers, such as the Gnielinski correlation [1]. These correlations are typically obtained under two assumptions: firstly, some kind of canonical boundary conditions (such as uniform heat flux or uniform external temperature), and secondly, fully developed conditions (indicating equilibrium between axial conduction and radial diffusion, both molecular and turbulent, and hence invariance of this balance in the axial direction). Removing the second constraint gives rise to the so-called turbulent *Graetz problem*, which studies how the temperature field responds to a step change in space to the temperature boundary condition, such as after entering a heated region; it is typically assumed that the velocity field is fully developed from the start (*thermally developing flow*). The length after which a particular quantity is indistinguishable from the fully developed state is called *thermal entry length* of that quantity; Notter and Sleicher [2] first reported the thermal entry length of the Nusselt number for a range of Pr and Re based on measured turbulent velocity profiles and an eddy diffusivity model for the turbulent heat flux. They observed that for Prandtl numbers greater than unity (such as for water), the entry length reduces with increasing Re (and is in the order of 5 diameters)[1], while the opposite is observed for very low Prandtl numbers (such as liquid metals, Pr $\leq$ 0.05): The entry length increases significantly with Re and only saturates at a much higher value, in the order of 30 diameters. This presents a challenge for the design of experiments for liquid metal heat transfer as well as for numerical studies.

---

[1]Notter and Sleicher [2] refer to the 5% thermal entry length, while we will report the 1% thermal entry length to keep consistency with [3]. These values may differ by a factor of 2-5, due to the exponential decay in the considered statistics, but will typically show the same trends when comparing between different cases.

In general, very few well-resolved numerical results of thermally developing internal flows have been reported. One relevant exception is the study of Rousta and Lessani [4] who reported statistics of thermally developing channel flow at $0.71 \leq \mathrm{Pr} \leq 7$ and $\mathrm{Re}_\tau = 180$. However, their domain is too short to even reach fully developed first-order statistics.

Recent numerical [5] and experimental [6] research has investigated the case of thermally fully developed flow with azimuthally non-uniform external heating, which is relevant e.g. for the design of concentrated solar power (CSP) plants. Both studies observed that the global Nu number is independent of the heat flux distribution around the circumference, which was a surprising observation given that the same is not true for channel flows. In section 2 we show that this observation is not a coincidence but can be shown analytically, including for the thermal entrance region. Hence we prove that the existing engineering correlations for the Nusselt number can also be applied to azimuthally inhomogeneous heating. Section 3 reports results from a well-resolved numerical database of the thermal entrance region for $\mathrm{Pr} = 0.025/0.71$ and $\mathrm{Re}_\tau = 180/550$, discussing the entry length of statistics of different order for uniform vs. non-uniform heating.

2 Theory and analysis

We consider a (hydrodynamically) fully developed pipe flow of a Newtonian fluid. The material properties of the fluid are assumed to be constant (in particular, independent of temperature), and temperature is modeled as a passive scalar. Viscous heating is neglected. Under these conditions, the conservation equation of temperature in cylindrical coordinates is given by [7] as

$$\rho c_p \left(\frac{\partial T}{\partial t} + u_r \frac{\partial T}{\partial r} + \frac{u_\varphi}{r} \frac{\partial T}{\partial \varphi} + u_z \frac{\partial T}{\partial z} \right) = \lambda \left[\frac{1}{r} \frac{\partial}{\partial r} \left(r \frac{\partial T}{\partial r} \right) + \frac{1}{r^2} \frac{\partial^2 T}{\partial \varphi^2} + \frac{\partial^2 T}{\partial z^2} \right] \tag{1}$$

with density ρ, specific heat at constant pressure c_p, and thermal conductivity λ. The instantaneous temperature field is subject to boundary conditions

$$\lim_{z \to -\infty} T(r, \varphi, z) = T_0, \quad \text{for a constant } T_0, \tag{2a}$$

$$\lambda \left. \frac{\partial T}{\partial r} \right|_R = \begin{cases} q_w(\varphi) & \text{for } \varphi \in [0, 2\pi) \text{ and } z \geq 0, \\ 0 & \text{for } \varphi \in [0, 2\pi) \text{ and } z < 0. \end{cases} \tag{2b}$$

These boundary conditions correspond to a uniform inlet temperature T_0 far away from the beginning of the heated section (eq. (2a)), and a prescribed heat flux on the outer wall of the pipe (eq. (2b)), which may or may not depend on φ. We assert that $q_w(\varphi) \not\equiv 0$, and that q_w is continuous and of bounded variation. Figure 1a illustrates the problem setup.

Equations (1) and (2b) are made dimensionless by introducing $\theta = 2U_b \rho c_p (T - T_0)/q_{w,\mathrm{ref}}$, $u_i = 2U_b u_i^*$, $z = Rz^*$, $r = Rr^*$, $t = 2R/U_b t^*$ and $\mathrm{Pe} = \rho c_p U_b 2R/\lambda$; where the bulk velocity is given by U_b and the pipe radius as R. Equation (1) then becomes, dropping star superscripts (which denote dimensionless quantities) for readability,

$$\left(\frac{\partial \theta}{\partial t} + u_r \frac{\partial \theta}{\partial r} + \frac{u_\varphi}{r} \frac{\partial \theta}{\partial \varphi} + u_z \frac{\partial \theta}{\partial z} \right) = \frac{1}{\mathrm{Pe}} \left[\frac{1}{r} \frac{\partial}{\partial r} \left(r \frac{\partial \theta}{\partial r} \right) + \frac{1}{r^2} \frac{\partial^2 \theta}{\partial \varphi^2} + \frac{\partial^2 \theta}{\partial z^2} \right] \tag{3}$$
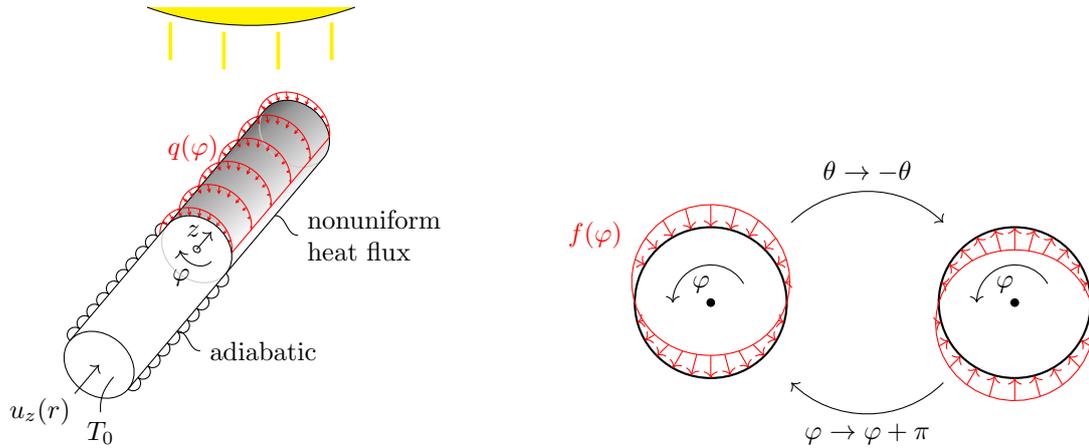
and the boundary conditions eqs. (2a) and (2b) are reformulated to

$$\lim_{z \to -\infty} \theta(r, \varphi, z) = 0, \tag{4a}$$

$$\left. \frac{\partial \theta}{\partial r} \right|_1 = Pe \begin{cases} f(\varphi) & \text{for } \varphi \in [0, 2\pi) \text{ and } z \geq 0, \\ 0 & \text{for } \varphi \in [0, 2\pi) \text{ and } z < 0; \end{cases} \tag{4b}$$

where $f(\varphi) = q_w(\varphi)/q_{w,\mathrm{ref}}$. The reference heat flux $q_{w,\mathrm{ref}}$ is given by $q_{w,\mathrm{ref}} := F[q_w]$ where F is a functional chosen according to the requirements listed below; we will use in the following

$$q_{w,\mathrm{ref}} := F[q_w] = \begin{cases} \overline{q_w} & \overline{q_w} \neq 0, \\ \sqrt{\frac{1}{\pi} \int_0^{2\pi} q_w(\varphi)^2 \mathrm{d}\varphi} & \overline{q_w} = 0 \end{cases} \tag{5}$$

(a) Sketch of the problem setup, modified from [3]

(b) Illustration of the transformation for the antisymmetry of the joint PDF

Figure 1: Problem setup

where $\overline{q_w} = 1/(2\pi) \int_0^{2\pi} q_w(\varphi)\mathrm{d}\varphi$. This satisfies four requirements:

$$\text{Nonzero:} \quad q_w \not\equiv 0 \ \Rightarrow\ F[q_w] \neq 0, \tag{6a}$$

$$\text{Mean consistency:} \quad \overline{q_w} \neq 0 \ \Rightarrow\ F[q_w] = \overline{q_w}, \tag{6b}$$

$$\text{Rotation invariance:} \quad F[q_w(\varphi)] = F[q_w(\varphi + \alpha)] \quad \text{for all } \alpha \in \mathbb{R}, \tag{6c}$$

$$\text{Homogeneity:} \quad \begin{cases} F[\alpha\, q_w] = \alpha\, F[q_w], & \text{if } \overline{q_w} \neq 0, \\ F[\alpha\, q_w] = |\alpha|\, F[q_w], & \text{if } \overline{q_w} = 0, \end{cases} \tag{6d}$$

the latter reflecting that linear homogeneity is incompatible with requiring both eqs. (6a) and (6c) for mean-free fields; instead we require absolute linear homogeneity for the zero-mean branch. The requirements are needed for (6a) avoiding division by zero, (6b) to match the standard definition of the global Nusselt number and (6d) an invariant dimensionless solution under scaling of the heat flux in physical dimensions, respectively.

The (dimensionless) bulk temperature is defined by

$$T_b = \frac{1}{RU_b} \int_0^R \overline{\langle Tu_z \rangle} r\mathrm{d}r, \quad \theta_b = 4 \int_0^1 \overline{\langle \theta u_z \rangle} r\mathrm{d}r \tag{7}$$

denoting with $\langle a \rangle$ the local statistical mean of a quantity a and with $\overline{a}$ the mean of a in the φ-direction (azimuthal mean). This gives rise to the global Nusselt number, i.e.

$$\mathrm{Nu}(z) = 2R \left.\overline{\frac{\partial \langle T \rangle}{\partial r}}\right|_R \frac{1}{\overline{\langle T_w \rangle} - T_b(z)} = \frac{2\mathrm{Pe}}{\overline{\langle \theta \rangle}|_{r=1} - \theta_b}, \quad z > 0, \tag{8}$$

where T_w is the wall temperature. The Nusselt number is therefore only a sensible measure if the azimuthal mean of the heat flux $\overline{q} = \lambda \left.\overline{\frac{\partial \langle T \rangle}{\partial r}}\right|_R$ is not zero.

2.1 Mean Nusselt number for azimuthally inhomogeneous heating

As discussed in the introduction, previous studies have observed that under thermally and hydraulically fully developed conditions, the global Nusselt number is insensitive to the distribution of the heat flux around the circumference (again noting that the Nusselt number is only defined if there is a nonzero mean heat flux).

The boundary condition $f(\varphi, t)$ is periodic in φ and can hence be expressed by means of a Fourier expansion. For a given velocity field $u_i(r, \varphi, z, t)$, the full solution for the temperature is, owing to the

linearity of the temperature equation, the sum of temperature responses to each wavenumber contribution of $f(\varphi)$. Hence, the statement can be proven by showing that for a boundary condition $\sin(k\varphi)$, $k > 0$, we find $\overline{\langle \theta u_z \rangle} = 0$ and $\overline{\langle \theta \rangle} = 0$ (the cosine case follows by a rotation of the coordinate system).

To prove this statement, we treat u_i and θ as random variables, and consider their joint probability density function (PDF), namely

$$p(u_r, u_\varphi, u_z, \theta, r, \varphi, z, t) \tag{9}$$

In particular, we are interested in azimuthal means of first moments of temperature, which are given by Pope [8]:

$$\overline{\langle u_i^m \theta \rangle}(r, z, t) = \iiint_{-\infty}^{\infty} \frac{1}{2\pi} \int_{-\infty}^{\infty} \int_0^{2\pi} u_i^m T p(u_r, u_\varphi, u_z, \theta, r, \varphi, z, t) \mathrm{d}\varphi \mathrm{d}\theta \mathrm{d}u_r \mathrm{d}u_\varphi \mathrm{d}u_z, \quad m \geq 0. \tag{10}$$

Consider $f(\varphi) = \sin(k\varphi)$ and $f'(\varphi) = -\sin(k\varphi)$. If $\theta(r, \varphi, z, t)$ solves eq. (1) with boundary condition f, then $-\theta(r, \varphi, z, t)$ solves eq. (1) with boundary condition f' for the same (fixed) velocity field. Thus, the joint PDF for f' is obtained from the joint PDF of f by flipping the sign of θ:

$$p'(u_r, u_\varphi, u_z, \theta, r, \varphi, z, t) = p(u_r, u_\varphi, u_z, -\theta, r, \varphi, z, t) \tag{11}$$

Moreover, rotating the coordinate system of the solution to f' by π/k yields the solution to f again; this is illustrated in fig. 1b. Hence:

$$p'(u_r, u_\varphi, u_z, \theta, r, \varphi + \pi/k, z, t) = p(u_r, u_\varphi, u_z, \theta, r, \varphi, z, t) \tag{12}$$

Both statements may be combined as

$$p(u_r, u_\varphi, u_z, -\theta, r, \varphi + \pi/k, z, t) = p(u_r, u_\varphi, u_z, \theta, r, \varphi, z, t), \tag{13}$$

which allows to compute eq. (10) by reducing the integration bounds in φ to $[0, 2\pi/k]$ (from the periodicity of the BC), splitting the remaining integral at π/k, substituting $\varphi \to \varphi + \pi/k$ and $\theta \to -\theta$ and finally using eq. (13).

$$\frac{1}{2\pi} \int_{-\infty}^{\infty} \int_0^{2\pi} u_i^m \theta p(u_j, \theta, r, \varphi, z, t) \mathrm{d}\varphi \mathrm{d}\theta = \frac{k}{2\pi} \int_{-\infty}^{\infty} \int_0^{\frac{2\pi}{k}} u_i^m \theta p(u_j, \theta, r, \varphi, z, t) \mathrm{d}\varphi \mathrm{d}\theta$$

$$= \frac{k}{2\pi} \left(\int_{-\infty}^{\infty} \int_0^{\frac{\pi}{k}} u_i^m \theta p(u_j, \theta, r, \varphi, z, t) \mathrm{d}\varphi \mathrm{d}\theta + \int_{-\infty}^{\infty} \int_0^{\frac{\pi}{k}} u_i^m \theta p(u_j, \theta, r, \varphi + \pi/k, z, t) \mathrm{d}\varphi \mathrm{d}\theta \right)$$

$$= \frac{k}{2\pi} \left(\int_{-\infty}^{\infty} \int_0^{\frac{\pi}{k}} u_i^m \theta p(u_j, \theta, r, \varphi, z, t) \mathrm{d}\varphi \mathrm{d}\theta - \int_{-\infty}^{\infty} \int_0^{\frac{\pi}{k}} u_i^m \theta p(u_j, -\theta, r, \varphi + \pi/k, z, t) \mathrm{d}\varphi \mathrm{d}\theta \right)$$

$$= \frac{k}{2\pi} \left(\int_{-\infty}^{\infty} \int_0^{\frac{\pi}{k}} u_i^m \theta p(u_j, \theta, r, \varphi, z, t) \mathrm{d}\varphi \mathrm{d}\theta - \int_{-\infty}^{\infty} \int_0^{\frac{\pi}{k}} u_i^m \theta p(u_j, \theta, r, \varphi, z, t) \mathrm{d}\varphi \mathrm{d}\theta \right) = 0$$

Consequently, the azimuthal mean of any first order moment in temperature (such as $\overline{\langle T \rangle}$ or $\overline{\langle T u_z \rangle}$) vanishes for a sinusoidal boundary condition, and by linearity of the temperature equation, those quantities can only depend on the mean of the boundary condition. Hence the Nusselt number – and all azimuthally averaged quantities in the mean temperature balance, are independent of the variation of the boundary condition $f(\varphi)$.

3 Numerical Setup and Results

In section 2, we have shown that the *azimuthally averaged* Nusselt number is independent of the heat flux distribution around the circumference, and hence also its thermal entry length. However, as described in [9], *pointwise* temperature statistics are strongly affected by inhomogeneous heating. In [3], we recently showed that nonuniform heating also increases the thermal entry length for laminar flow. One-sided heating, in particular, was shown to delay the onset of the fully developed state significantly. In this section, we extend these results to turbulent flow by means of numerical simulations.

The turbulent flow database is obtained using NekRS [10], a portable version of the classical spectral element solver Nek5000. The mesh is reused from [9] and extended in the axial direction, preserving axial
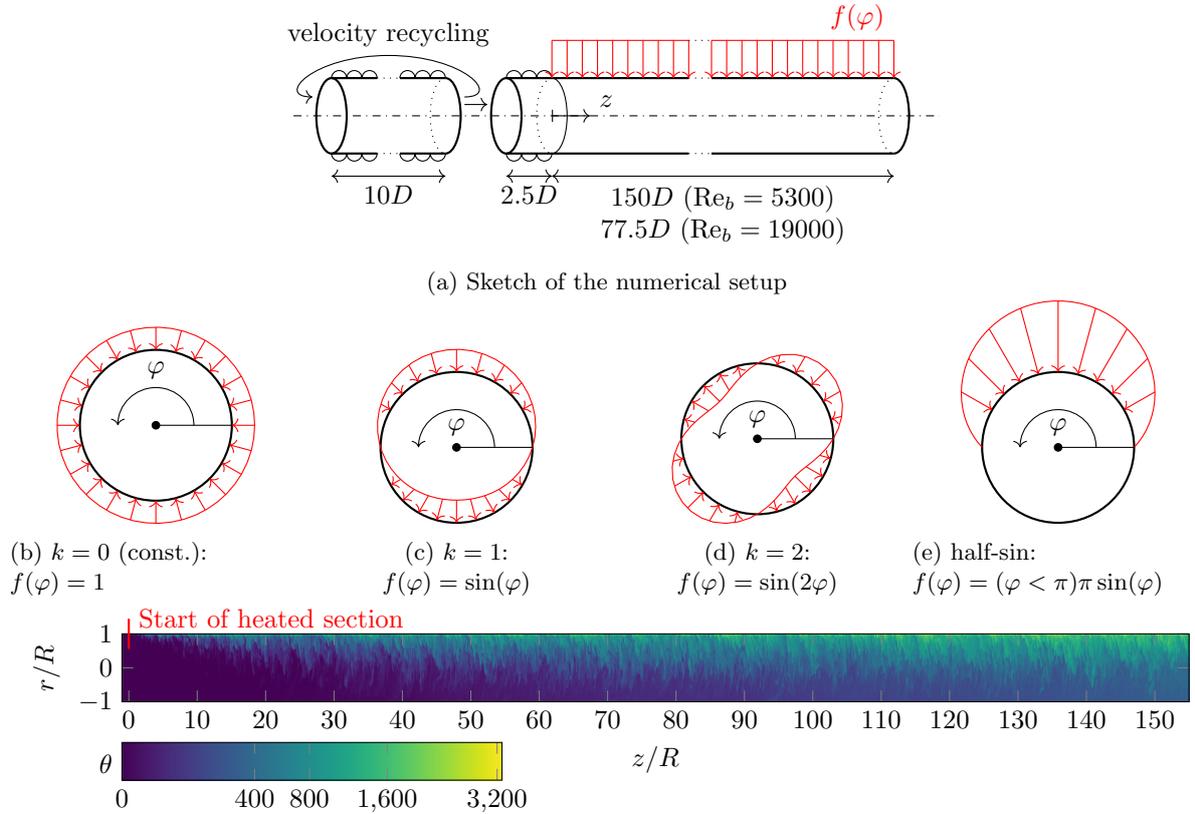
(a) Sketch of the numerical setup

(b) $k = 0$ (const.):
$f(\varphi) = 1$

(c) $k = 1$:
$f(\varphi) = \sin(\varphi)$

(d) $k = 2$:
$f(\varphi) = \sin(2\varphi)$

(e) half-sin:
$f(\varphi) = (\varphi < \pi)\pi \sin(\varphi)$

(f) An r-z slice of the instantaneous dimensionless temperature for Pr = 0.71, $\mathrm{Re}_b = 19000$, half-sinusoidal heating. The horizontal axis is compressed by a factor of 5 to fit the page.

Figure 2: Illustration of the setup. Note that in figs. 2b to 2e the direction of the arrows relative to the outward-pointing normal vector distinguishes heating and cooling.

resolution; see [9] for the validation. The simulation is hence a well-resolved LES for the velocity, which fully resolves the scales of temperature. As in [9], the necessary additional dissipation is provided by the approximate deconvolution method.

A periodic precursor simulation with length $L = 10D$ is used to generate a fully developed velocity field, which is sufficient according to [11]. The flow in the periodic subregion has a constant flow rate. The flow then enters the heated section, which has a length of $150D$ for the $\mathrm{Re}_b = 5300$ ($\mathrm{Re}_\tau \approx 180$) case and a length of $77.5D$ for the $Re_\tau = 19000$ ($\mathrm{Re}_\tau \approx 550$) case. This setup is illustrated in fig. 2a

Four different boundary conditions are considered, sketched in figs. 2b to 2e. Two of those – constant and half-sinusoidal – have the same, nonzero azimuthal mean. Their $\mathrm{Nu}(z)$ may be readily evaluated according to eq. (8), which is displayed in fig. 3. As expected from the derivation in section 2, both cases yield the same Nusselt number for all z.

As in the laminar case [3], the thermal entry length of the pointwise mean temperature can be much longer than that of the Nusselt number, in particular in case of inhomogeneous heating. The scenario posed by the half-sinusoidal boundary condition is too complex for an intuitive evaluation of these lengths, hence we note that the mean temperature can be computed by superposition of the responses to the wavenumbers in the spectrum of the boundary condition. Therefore, we turn our attention to the $k = 1$ and $k = 2$ cases (cf. figs. 2c and 2d). We observe in the numerical data that the mean temperature response to a boundary condition with only a single azimuthal wavenumber (monochromatic boundary condition) ($k = 1$ or $k = 2$) very closely matches $\langle\theta\rangle = f(\varphi)\hat{\theta}(r, z)$, i.e. the only azimuthal wavenumber present in the mean temperature field is that of the boundary condition itself; the energy associated with other azimuthal wavenumbers of the mean temperature is more than four order of magnitudes below that
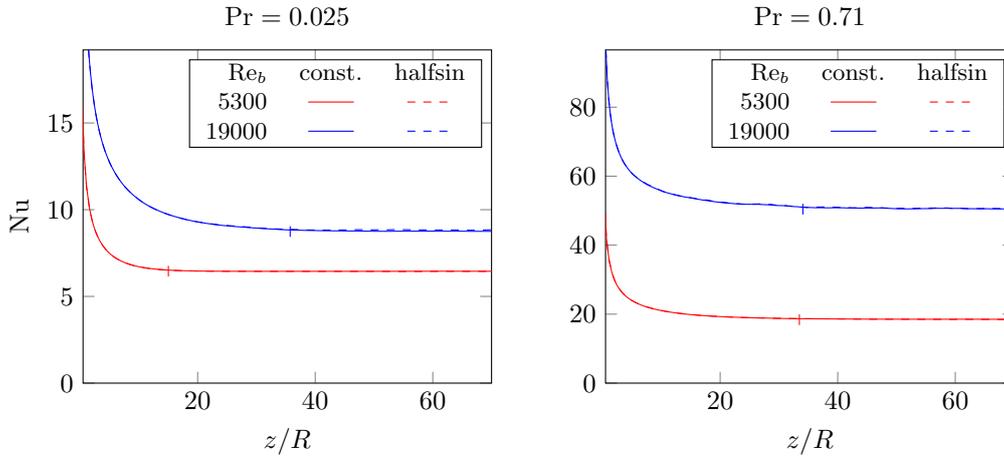
Figure 3: Nusselt number as function of z for (left) $\mathrm{Pr} = 0.025$ and (right) $\mathrm{Pr} = 0.71$ at $\mathrm{Re}_b = 5300, 19000$ for both constant and half-sinusoidal heating. The position of the markers (small vertical lines) indicates the 1% thermal entry length.

of k, which is comparable with the statistical uncertainty. Consequently, the local Nusselt number

$$\mathrm{Nu}_l(z, \varphi) = \frac{2\mathrm{Pe}\, f(\varphi)}{\langle \theta_w \rangle(\varphi) - \theta_b(z, \varphi)} \quad z > 0 \tag{14}$$

is constant over the azimuthal coordinate (although for practical purposes, the evaluation does not consider values near the roots of the boundary condition), and can be taken as a practical measure for evaluating the development length of the point-wise temperature for non-uniformly heated cases.

For the considered cases with monochromatic boundary condition, the mean local Nusselt number is displayed in fig. 4. It is immediately clear that for all pairs of Pr and Re_b, half-sided heating ($k = 1$) reaches the fully developed state much later than the homogeneous case (almost by a factor of four in the $\mathrm{Re}_b = 5300$ case), while the development length of $k = 2$ falls in between those two. The same trend was observed in the laminar case [3], and we would therefore expect that the temperature field in response to higher k has a further reduced entry length, like in the laminar case. In other words, the thermal entry length of the *pointwise* temperature field responding to a composite boundary condition is dominated by its $k = 1$ component, followed by $k = 0$ and $k = 2$; high wavenumber modes only play a minor role in the overall development length.

We also observe that the values of Nu_l are not monotonic in k; indeed in the fully developed regime we consistently find

$$\overline{\mathrm{Nu}_{l,k=1}} < \overline{\mathrm{Nu}_{l,k=0}} < \overline{\mathrm{Nu}_{l,k=2}} \tag{15}$$

for all Re and Pr examined.

This trend can be understood by viewing Nu_l as a measure of the uniformity of the temperature profile along a radial line, after normalization of the wall gradient.[2] When k increases, the hot and cold lobes of the heat flux move closer together, leading to the core of the pipe becoming increasingly isothermal (and hence Nu_l increases). For $k = 0$, the radial heat flux at the center is zero by symmetry; for $k = 1$ it is not, i.e. $\frac{\partial T}{\partial r}\big|_{r=0} \neq 0$. This central heat flux makes the temperature profile less uniform than that for $k = 0$.

A comparison with laminar flow supports this analysis. Using the fully developed solution by [3] we obtain

$$\overline{\mathrm{Nu}_{l,k=0}} = \frac{48}{11} \approx 4.36, \quad \overline{\mathrm{Nu}_{l,k}} = (2k^2 + 12k + 16)/(k + 6) \quad (k > 0) \tag{16}$$

which gives $\overline{\mathrm{Nu}_{l,k=1}} \approx 4.28$, $\overline{\mathrm{Nu}_{l,k=2}} = 6$, $\overline{\mathrm{Nu}_{l,k=3}} \approx 7.78$ and $\overline{\mathrm{Nu}_{l,k=4}} = 9.6$. Clearly, these values show the same non-monotonic behavior that was observed in the turbulent cases.

---

[2] This explanation neglects $\langle u'_z \theta' \rangle$, whose contribution to θ_b is however two orders of magnitude smaller than that of $\langle u_z \rangle \langle \theta \rangle$ for all considered cases.
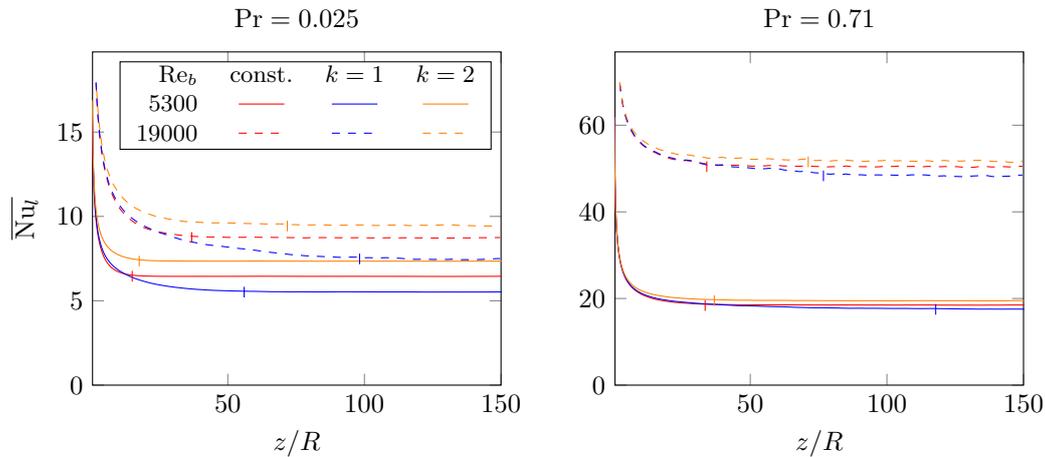
Figure 4: Azimuthal mean of the local Nusselt number as a function of z for (left) $\mathrm{Pr} = 0.025$ and (right) $\mathrm{Pr} = 0.71$ at $\mathrm{Re}_b = 5300, 19000$ (linestyle) for azimuthal heating modes (colored) $k = 0$ (constant), $k = 1$ and $k = 2$. Additionally marked is the 1% thermal entry length of these quantities.

4 Conclusion

In this contribution, we have presented a well-resolved numerical database of the thermal inlet in turbulent pipe flows, subject to both azimuthally homogeneous and inhomogeneous heat flux. We have shown that the global heat transfer coefficient (Nu) is not affected by inhomogeneous heating: both from an analytical perspective and based on the numerical data. Hence, existing $\mathrm{Nu} = f(\mathrm{Re}, \mathrm{Pr})$ correlations keep their validity for the case of inhomogeneous boundary conditions.

We have further shown that the (pointwise) thermal entry length of the mean temperature depends greatly on the heat transfer distribution. In particular, one-sided heating (azimuthal wavenumber $k = 1$) is shown to delay the thermal entry by a factor of up to four.

References

[1] Volker Gnielinski. Neue Gleichungen für den Wärme- und den Stoffübergang in turbulent durchströmten Rohren und Kanälen. *Forschung im Ingenieurwesen A*, 1975.

[2] Robert H. Notter and Charles A. Sleicher. A solution to the turbulent Graetz problem—III Fully developed and entry region heat transfer rates. *Chemical Engineering Science*, 27(11):2073–2093, 1972.

[3] Jonathan Neuhauser, Jan-Henrik Metsch, Davide Gatti, and Bettina Frohnapfel. Solution of the extended Graetz problem for nonuniform heat flux. *International Journal of Heat and Mass Transfer*, 249:127198, October 2025.

[4] Farid Rousta and Bamdad Lessani. Numerical study of thermally developing turbulent internal flows. *International Journal of Heat and Mass Transfer*, 188:122623, June 2022.

[5] Steffen Straub, Pourya Forooghi, Luca Marocco, Thomas Wetzel, and Bettina Frohnapfel. Azimuthally inhomogeneous thermal boundary conditions in turbulent forced convection pipe flow for low to medium Prandtl numbers. *International Journal of Heat and Fluid Flow*, 77:352–358, June 2019.

[6] Tim Laube, Benjamin Dietrich, Luca Marocco, and Thomas Wetzel. Turbulent heat transfer in a liquid metal tube flow with azimuthally inhomogeneous heat flux. *International Journal of Heat and Mass Transfer*, 189:122734, June 2022.

[7] R. Byron Bird, Warren E. Stewart, and Edwin N. Lightfoot. *Transport Phenomena*. John Wiley & Sons, Inc., New York, revised second edition edition, 2007.

[8] Stephen B. Pope. *Turbulent Flows*. Cambridge University Press, Cambridge ; New York, 2000.

[9] Steffen Straub, Pourya Forooghi, Luca Marocco, Thomas Wetzel, Ricardo Vinuesa, Philipp Schlatter, and Bettina Frohnapfel. The influence of thermal boundary conditions on turbulent forced convection pipe flow at two Prandtl numbers. *International Journal of Heat and Mass Transfer*, 144:118601, December 2019.

[10] Paul Fischer, Stefan Kerkemeier, Misun Min, Yu-Hsiang Lan, Malachi Phillips, Thilina Rathnayake, Elia Merzari, Ananias Tomboulides, Ali Karakus, Noel Chalmers, and Tim Warburton. NekRS, a GPU-accelerated spectral element Navier–Stokes solver. *Parallel Computing*, 114:102982, December 2022.

[11] Sergio Pirozzoli, Joshua Romero, Massimiliano Fatica, Roberto Verzicco, and Paolo Orlandi. One-point statistics for turbulent pipe flow up to $\mathrm{Re}_\tau \approx 6000$. *Journal of Fluid Mechanics*, 926:A28, November 2021.